Supplemental Materials

Molecular Biology of the Cell

Bestul et al.

SUPPLEMENTAL MATERIALS

SUPPLEMENTAL RESULTS

Most biochemical properties of ScPFY(9-Mut) are more similar to WT ScPFY than to SpPRF.
The stability of the purified profilins was determined by measuring their intrinsic tryptophan fluorescence upon urea denaturation (Supplemental Figure 3A). The stability of ScPFY(9-Mut) ($D_{1/2}$ = 2.6 M urea) is not significantly different from WT ScPFY (3.3 M urea), which are both less stable than SpPRF (4.5 M urea) (Lu and Pollard, 2001; Ezezika *et al.*, 2009).

Despite altering nine residues in and around the actin-binding region, ScPFY(9-Mut)'s interaction with actin monomers is similar to WT ScPFY. The affinity for muscle Mg-ATP-actin monomers, determined by their ability to prevent spontaneous actin assembly, is similar between ScPFY(9-Mut) (K_d = 0.4 μM), WT ScPFY (0.7 μM) and SpPRF (0.8 μM) (Supplemental Figure 3B and C). Profilin's ability to bind fission yeast actin was investigated by incubating fission yeast extracts supplemented with PLP-coated sepharose beads and a range of purified profilin concentrations (Supplemental Figure 3D and E). Both ScPFY(9-Mut) and WT ScPFY 'pull down' more actin associated with PLP-beads from fission yeast extracts than does SpPRF. Finally, both ScPFY(9-Mut) and WT ScPFY increase the nucleotide exchange rate of muscle actin monomers significantly more than SpPRF (Supplemental Figure 3F and G).

Profilin's affinity for PLP (Supplemental Figure 4A) and Cdc12(FH1) (Supplemental Figure 4B) was determined by measuring profilin's increase in intrinsic tryptophan fluorescence upon complex formation. Since amino acids were not altered in the region of profilin that binds proline-rich ligands (Supplemental Figure 1A and B), it is not surprising that ScPFY(9-Mut) and WT ScPFY bind similarly to proline rich ligands. ScPFY(9-Mut) and WT ScPFY bind to PLP (195 and 224 μM, respectively) and Cdc12(FH1) (22.7 and 24.7 μM, respectively) approximately 3.5-fold less tightly than SpPRF binds to PLP (59 μM) and Cdc12(FH1) (6.4 μM) (Eads *et al.*, 1998; Lu and Pollard, 2001; Neidt *et al.*, 2009; Scott *et al.*, 2011).

The ability of profilin to bind the phosphoinositide PtdIns(4,5)P_2 was determined by incubating profilins with a range of PtdIns(4,5)P_2 micelle concentrations and spinning the mixtures through 30 kDa cut-off filter that permits only free profilin to pass through (Supplemental Figure 4C). ScPFY(9-Mut) binds PtdIns(4,5)P_2 micelles 2-fold better than SpPRF, and 5-fold better than WT ScPFY. ScPFY(9-Mut)'s higher affinity for PtdIns(4,5)P_2 might be explained by the addition of a positive residue (A84K) in the PtdIns(4,5)P_2-binding region (Sohn *et al.*, 1995; Chaudhary *et al.*, 1998; Lu and Pollard, 2001).

Table S1. List of ScPFY Mutants Identified by Complementation Selection

Mutant #	Mutations Present
V12	T32A, N52D, N59T, M69I
V13	A28S, T32A, A54P, L56M, S58G, L70T, H82L, Q94L, A107P, T111A, V114T
V14	A28S, N52D, M69I, L70T, D75G, Q106L
V15	T32A, M69I, L70T, D75G, H82L, Q94L
V16[a]	N52D, M69I, H82L
V17	T32A, M69I, D75G, H82L
V18	T32A, N52D, M69I, D75G, H82L, Q94L, A107P
V19	A28S, T32A, N52D, S58G, M69I, L70T, D75G, Q106L
V110	A28S, M69I, D75G, H82L, Q106T
V21	A28S, N52D, L56M, M69I, L70T, H82L, V114T
V22	A28S, T32A, L56M, M69I, L70T, Q94L, V114T
V23	A28S, N52D, L56M, N59T, M69I, L70T, D75G, V114T
V31	A54P, S58G, M69I, D75G, H82L, Q94L, Q106L, A107P, V114T
V35	L56M, N59T, M69I, H82L, Q94L, Q106L, T111A
V39	A54P, S58G, M69I, D75G, H82L, A107P, V114T
V310	N59T, M69I, D75G
V311	N59T, M69I, H82L, A107P, V114T

[a]The N52D, M69I, H82L mutant was isolated twice.

Table S2. Frequency of Mutations in ScPFY Mutants

Mutations	# of Appearances (17 total)
A28S	7
T32A	7
N52D	7
A54P	3
L56M	5
S58G	4
N59T	5
M69I	16
L70T	7
D75G	10
H82L	11
Q94L	6
Q106L	5
A107P	5
T111A	2
V114T	7

Table S3. Strains Used in this Study

Strain Name	Genotype	Reference
FY527	h-, leu1-32, his3-D1, ura4-D18, ade6-M216	(Liang *et al.*, 1999)
FY528	h+, leu1-32, his3-D1, ura4-D18, ade6-M210	(Liang *et al.*, 1999)
KGY491	h+, cdc3-124, leu1-32, ura4-D18, ade6-M216	(Balasubramanian *et al.*, 1996)
FY10	h-, ura4-294	(Keeney and Boeke, 1994)
KV354	h-, rlc1-GFP-KanMX6, leu1-32, ura4-D18, ade6-M216	(Le Goff *et al.*, 2000)
KV614	h+, cdc3-124, rlc1-GFP-KanMX6, leu1-32, ura4-D18, ade6-M216	This study
KV624	h+, cdc3-124, pAct1-Lifeact-mCherry::Leu1+, leu1-32, ura4-D18, ade6-M216	This study
KV629	h-, ura4-294, Pnmt81-SpPRF::Ura4+	This study
KV630	h-, ura4-294, Pnmt81-ScPFY::Ura4+	This study
KV631	h-, ura4-294, Pnmt81-ScPFY(9-Mut)::Ura4+	This study
KV643	h?, cdc3-124, rlc1-GFP-KanMX6, Pnmt81-SpPRF::Ura4+, ura4-294	This study
KV644	h?, cdc3-124, rlc1-GFP-KanMX6, Pnmt81-ScPFY::Ura4+, ura4-294	This study
KV645	h?, cdc3-124, rlc1-GFP-KanMX6, Pnmt81-ScPFY(9-Mut)::Ura4+, ura4-294	This study
FC1141	h-, GFP-Syb1::KanMX6, ade6-, leu1-	(Basu and Chang, 2011)
KV789	h?, cdc3-124, GFP-Syb1::KanMX6, ade6-, leu1-	This study

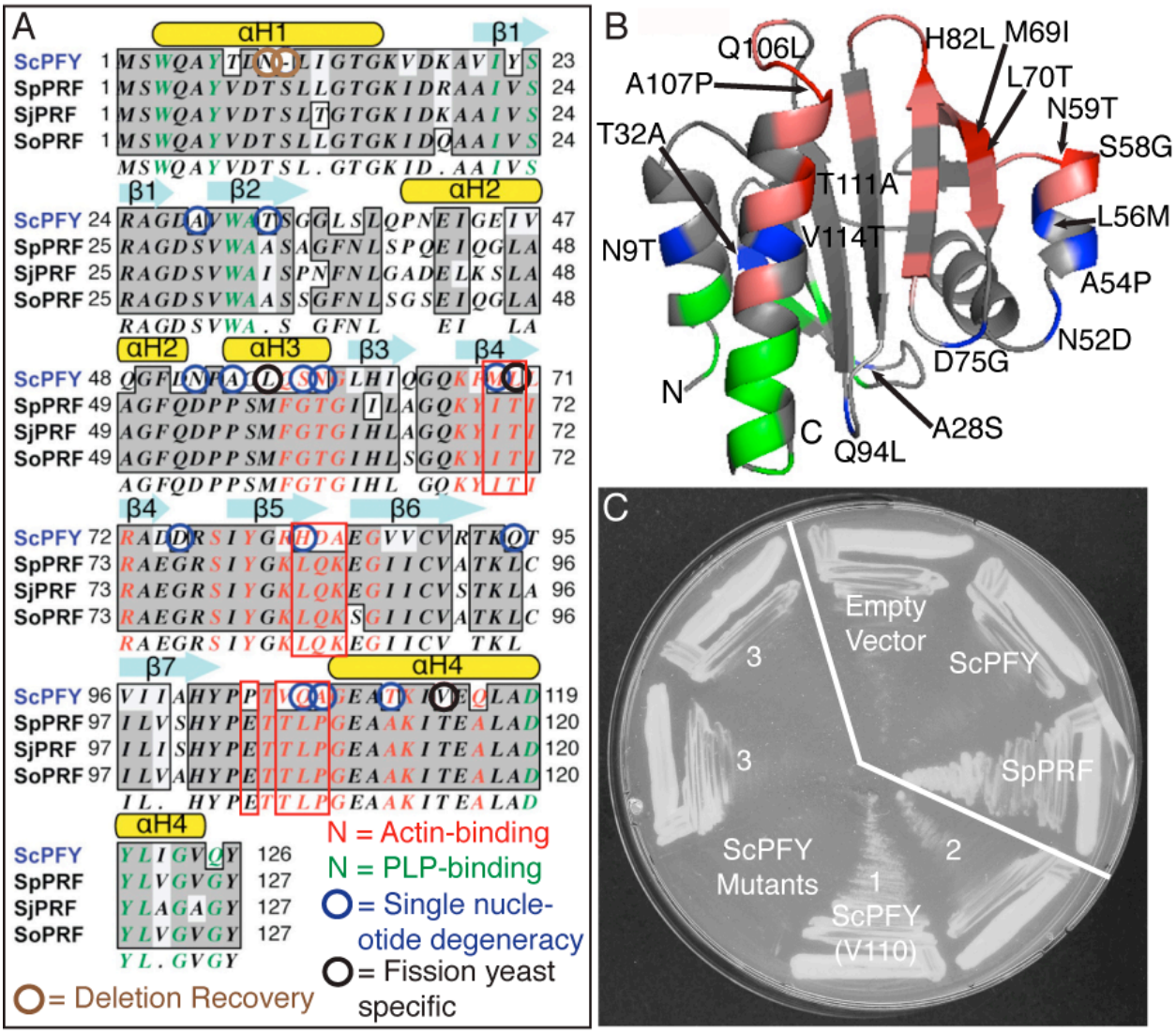

Supplemental Figure 1. Selection of a ScPFY mutant library created by directed random mutagenesis. (A) Sequence alignment of budding yeast profilin (ScPFY, AAA34861) and three *Schizosaccharomyces* profilins (SpPRF, NP593827; SjPRF, EEB09758; SoPRF, SOCG00766). Residues in red and green are in the actin and poly-L-proline binding regions (Lu and Pollard, 2001). Circled residues were selected for mutagenesis, because they are specific to the fission yeast genus (black circles), single nucleotide degeneracy (blue circles), or corrected a deleted/missing ScPFY residue (brown circles). Residues boxed in red constitute the nine mutations in ScPFY(9-Mut). Secondary structures are indicated above the primary sequence with yellow ovals (α-helix) and light blue arrows (β-sheets). (B) Structure of ScPFY (Eads *et al.*, 1998) with residues highlighted in red (actin binding), green (poly-L-proline binding), pink (actin binding and selected for mutation), and blue (not in a known ligand-binding region, but selected for mutagenesis). (C) Representative plate from selection of the ScPFY mutant library. Profilin mutant *cdc3-124* cells expressing WT and ScPFY mutants from a plasmid under the control of the *nmt81* promoter, grown at 25°C for 2 days and then 36°C for 2 days. ScPFY mutants were ranked from 1 to 3: 3, similar to WT ScPFY; 2, moderate complementation; 1, similar to SpPRF. The strain ranked 1 in this example is ScPFY mutant V110 (A28S, M69I, D75G, H82L, Q106T).

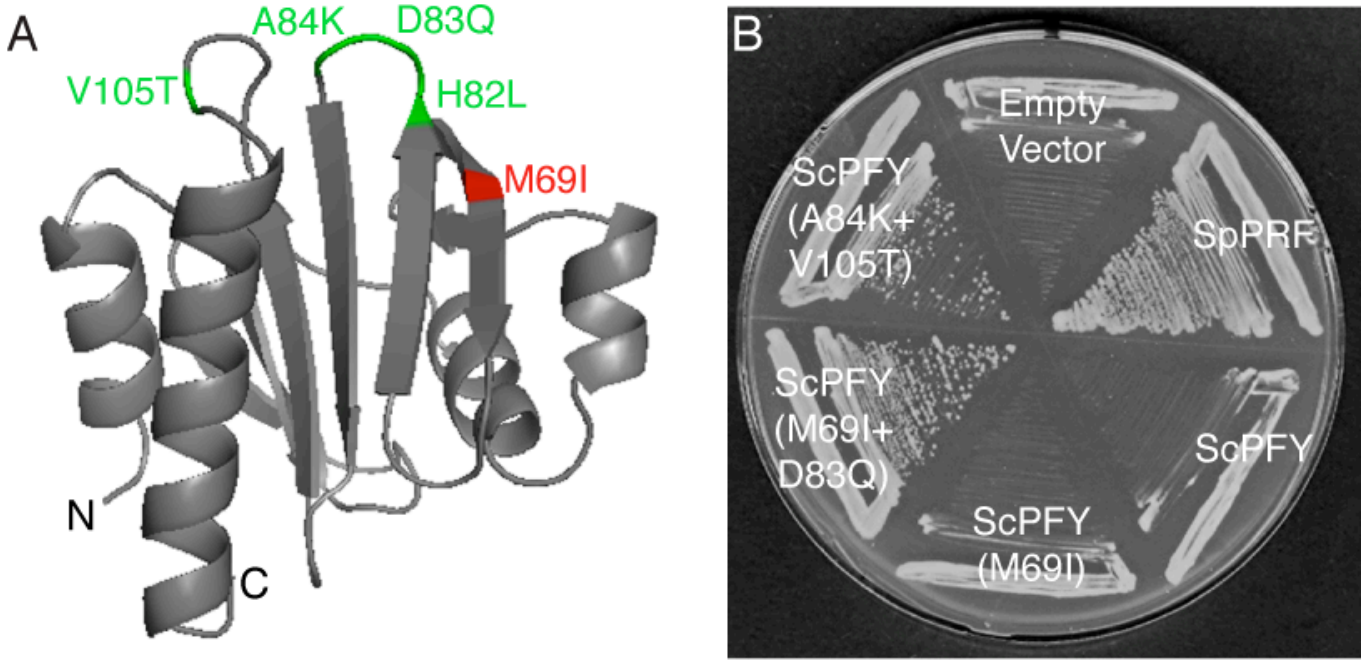

Supplemental Figure 2. ScPFY(M69I) is not necessary or sufficient for complementation of *cdc3-124* cells. (A) Structure of ScPFY (Eads *et al.*, 1998) with the M69I mutation indicated in red and other mutations in the actin-binding region found to be important for *cdc3-124* complementation highlighted in green. (B) Fission yeast profilin *cdc3-124* cells after 3 days at 36°C with either an empty vector, or a vector expressing the indicated ScPFY mutants under control of the *nmt81* promoter.

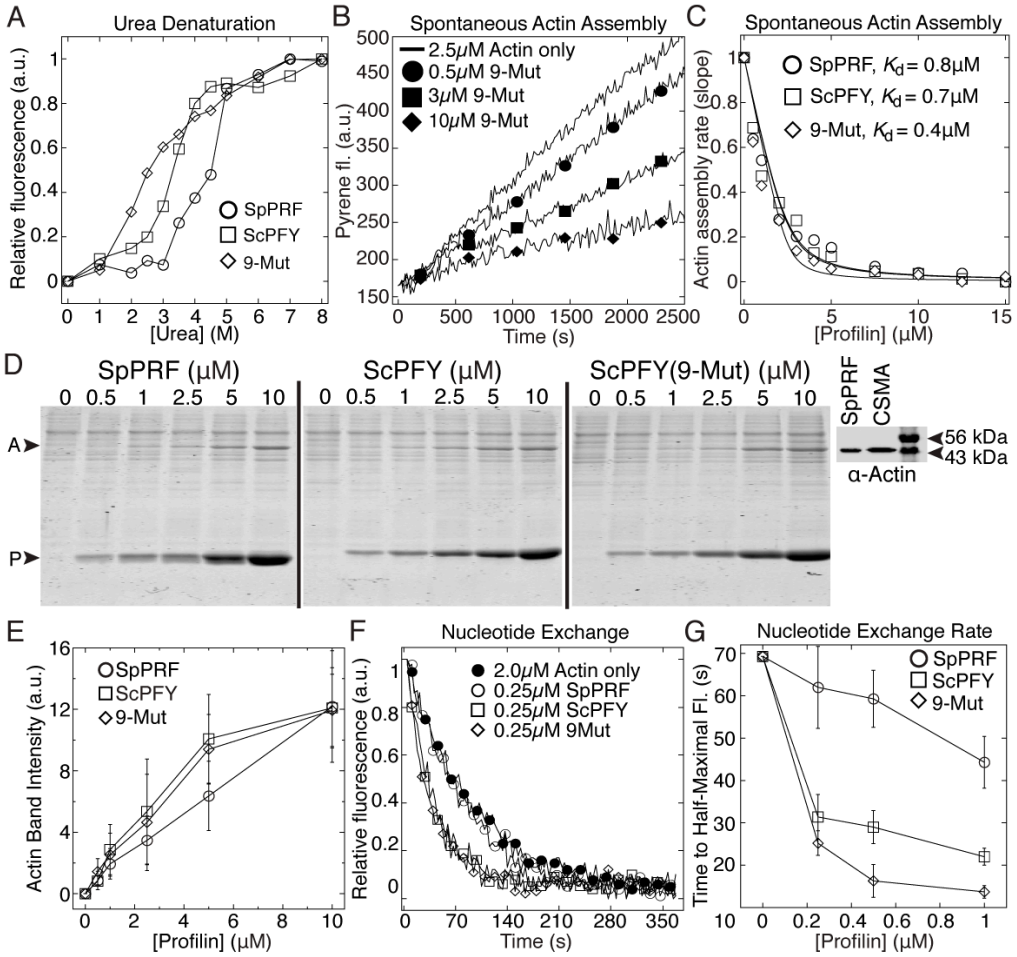

Supplemental Figure 3. Actin-binding properties of ScPFY(9-Mut). (A) Urea denaturation of purified profilins assayed by intrinsic fluorescence. Dependence of 370 nm fluorescence emission on the concentration of urea for 1.0 μM of the indicated profilins: SpPRF (○), WT ScPFY (□) and ScPFY(9-Mut) (◇). (B-C) Binding of profilins to muscle actin monomers. Spontaneous assembly of 2.5 μM Mg-ATP muscle actin monomers (20% pyrene-labeled) over a range of concentrations of the indicated profilins. (C) Dependence of the actin assembly rate (slope) on the concentration of profilin. Curve fits revealed equilibrium dissociation constants of 0.8 μM for SpPRF (○), 0.7 μM for WT ScPFY (□) and 0.4 μM for ScPFY(9-Mut) (◇). (D-E) Binding of profilins to fission yeast actin. Fission yeast cell extracts were incubated with 25 μL bed volume PLP-Sepharose beads and a range of purified profilin concentrations. (D) (Left) Coomassie Blue-stained 15% SDS-PAGE gels of proteins pulled down by PLP-Sepharose beads. Labeled arrowheads indicate actin (A) and profilin (P) bands. (Right) Western blot with anti-actin antibody verifies that the indicated band is actin. SpPRF lane is cell extract incubated with SpPRF. Purified chicken skeletal muscle actin (CSMA) provides a positive control. (E) Dependence of the normalized amount of actin pulled down on the concentration of SpPRF (○), WT ScPFY (□) and ScPFY(9-Mut) (◇). Error bars = s.d., n = 3. (F-G) Nucleotide exchange of 2 μM εATP muscle actin catalyzed by profilin. (F) Loss of 2 μM εATP muscle actin fluorescence over time in the absence (●) or presence of 0.25 μM SpPRF (○), WT ScPFY (□) or ScPFY(9-Mut) (◇). (G) Rate of nucleotide exchange (time of half-maximal εATP fluorescence) over a range of SpPRF (○), WT ScPFY (□) and ScPFY(9-Mut) (◇) concentrations. Error bars = s.d., n = 3.

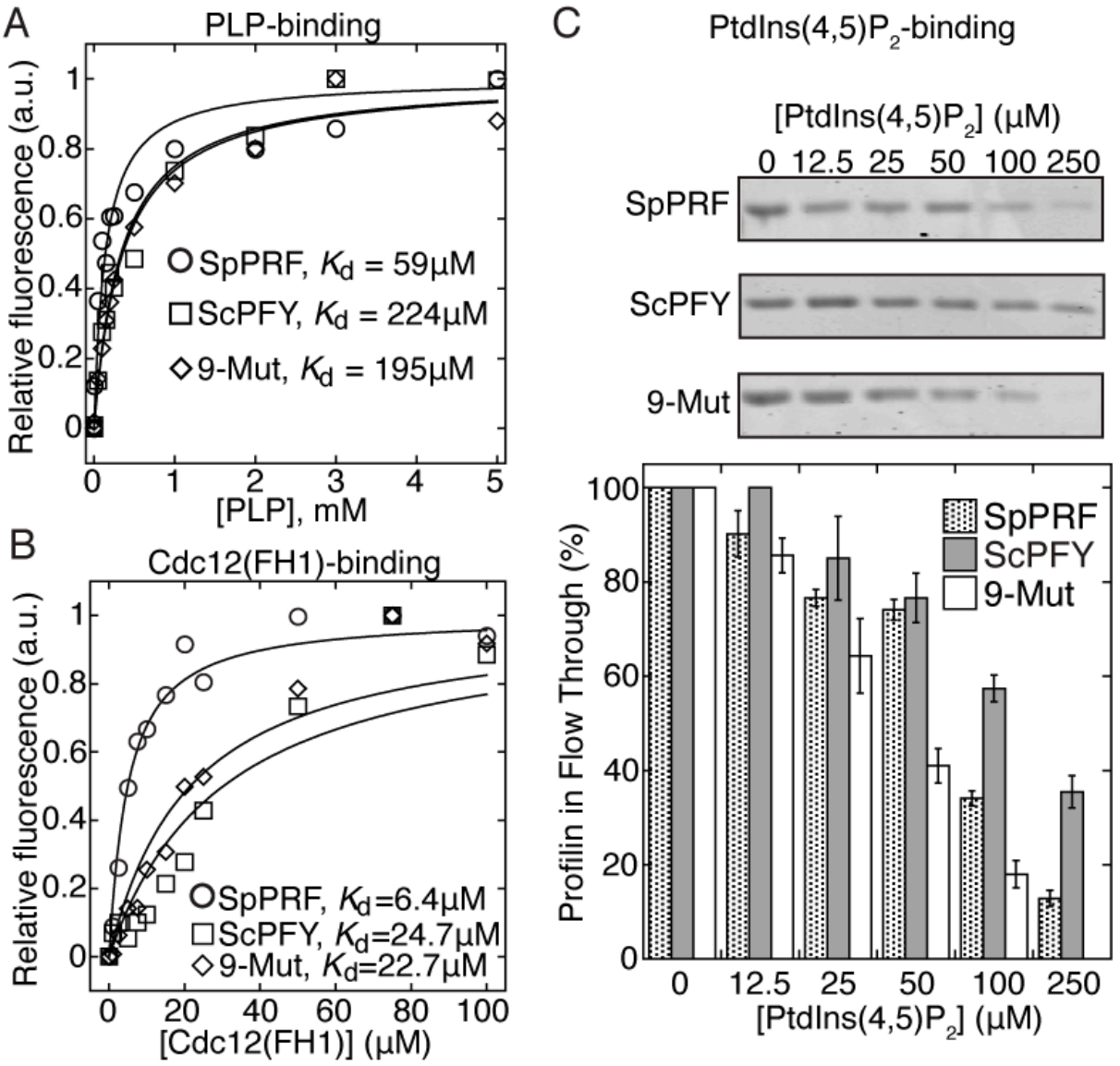

Supplemental Figure 4. Poly-L-proline-, FH1-, and PIP_2-binding properties of ScPFY(9-Mut). (A) Binding of profilins to poly-L-proline (PLP). Curve fits of the dependence of profilin's intrinsic tryptophan fluorescence on the concentration of PLP revealed equilibrium dissociation constants of 59 μM for SpPRF (○), 224 μM for WT ScPFY (□) and 195 μM for ScPFY(9-Mut) (◇). (B) Binding of profilins to the formin Cdc12 FH1 domain by tryptophan fluorescence. Curve fits revealed equilibrium dissociation constants of 6.4 μM for SpPRF (○), 24.7 μM for WT ScPFY (□) and 22.7 μM for ScPFY(9-Mut) (◇). (C) Binding of profilins to PtdIns(4,5)P_2. The indicated concentrations of PtdIns(4,5)P_2 micelles were incubated with 5 μM profilin and spun through a 30,000 Da molecular weight cut-off filter. (Top) The flow-through was run on a 15% SDS-PAGE gel. (Bottom) Plot of the average percentage of SpPRF (dotted), WT ScPFY (grey) and ScPFY(9-Mut) (white) present in the flow-through. Error bars = s.d., n = 3.

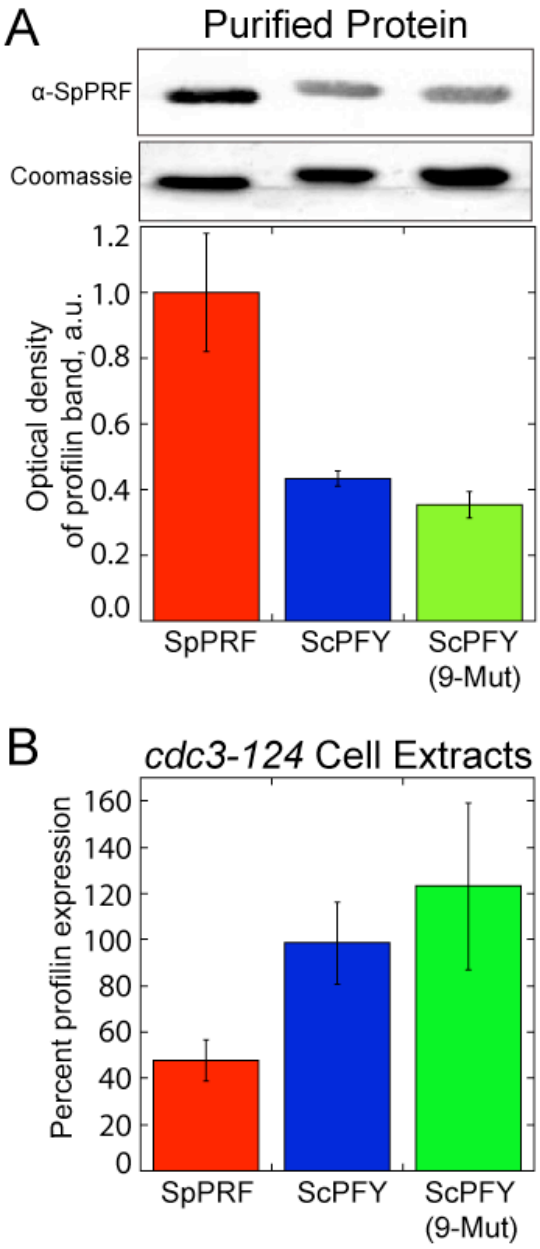

Supplemental Figure 5. Expression of SpPRF, ScPFY, and ScPFY(9-Mut) in fission yeast cells. Western blot analysis with α-SpPRF antibody. (A) Blot (top) and corresponding Coomassie-blue stained gel (middle) of 1.0 µg purified recombinant SpPRF, ScPFY, or ScPFY(9-Mut). (Bottom) Densitometry of bands from blots. Error bars = s.d., n = 3. (B) The percent that SpPRF, ScPFY or ScPFY(9-Mut) are expressed from the *P81nmt1* promoter in *cdc3-124* cells, compared to the expression of SpPRF in wild type cells. Expression levels were determined by blotting extracts with α-SpPRF. Values are normalized to the relative reactivity of α-SpPRF to the purified recombinant proteins in (A). Error bars = s.d., n = 3.

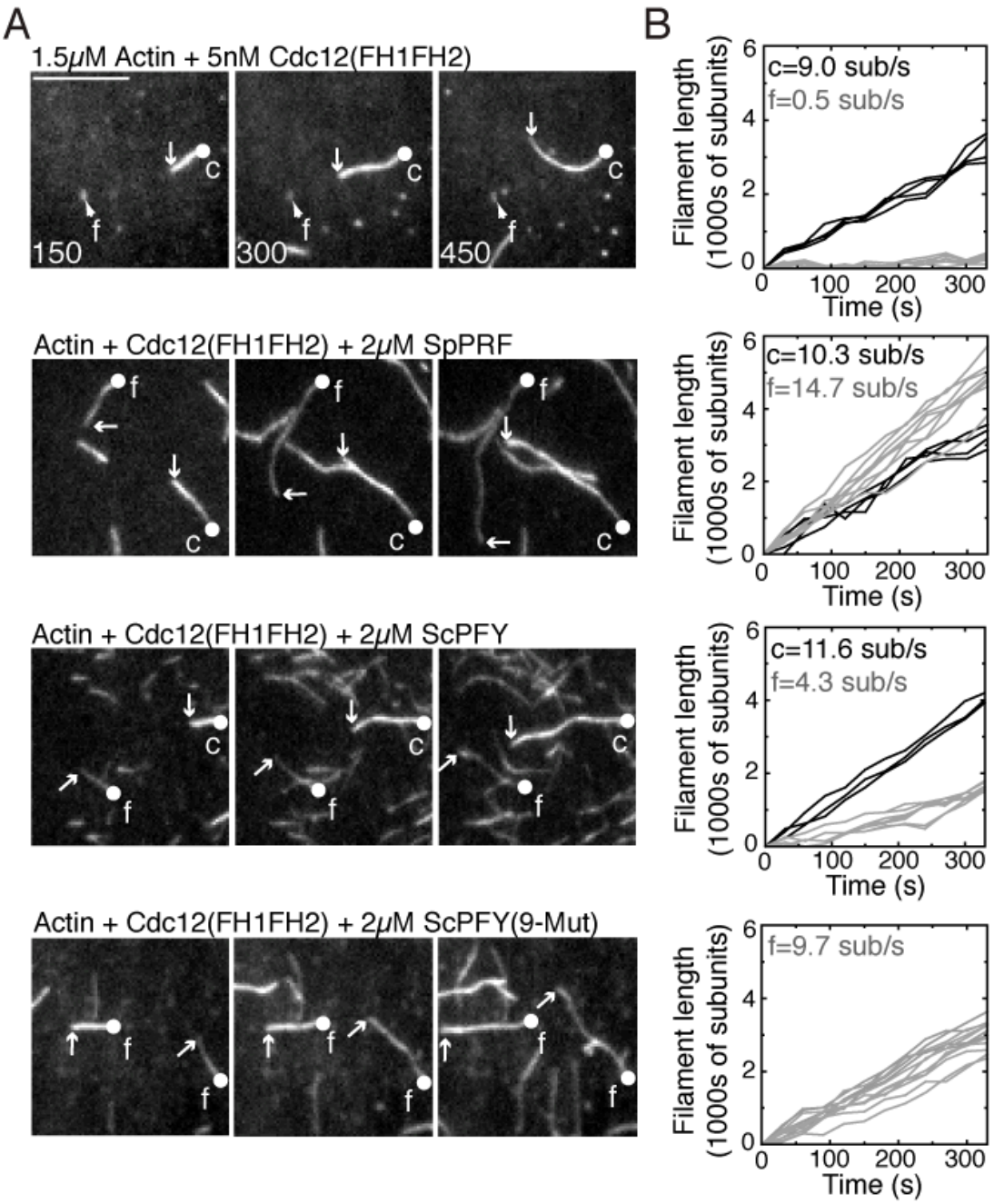

Supplemental Figure 6. Formin Cdc12-associated filaments elongate faster with ScPFY(9-Mut) than WT ScPFY. TIRF microscopy visualization of the spontaneous assembly of unlabeled 1.0 μM Mg-ATP actin with 0.5 μM Mg-ATP actin labeled with Oregon green and the indicated combinations of 5 nM formin Cdc12(FH1FH2) and 2 μM profilin (Supplemental Videos 3-6). (A) Micrographs of individual actin filaments over time. Scale bar = 10 μm. Control (c) and formin-associated (f) filaments are labeled. Barbed and pointed ends are labeled with white circles and arrows. Time in seconds is indicated in the lower left corner. (B) Plots of the length of individual filaments over time in the presence of 2.5 nM Cdc12(FH1FH2) alone, or Cdc12(FH1FH2) and 2 μM SpPRF, WT ScPFY, or ScPFY(9-Mut). Control filaments (c) are denoted by black lines and formin-associated filaments (f) are denoted by grey lines, with the indicated average elongation rates (subunits s^{-1}).

SUPPLEMENTAL VIDEOS

Video 1. Contractile ring kinetics in WT and *cdc3-124* cells. Related to Figure 3A. Time-lapse (in minutes) of a single Z-plane of a WT or *cdc3-124* cell expressing Rlc1-GFP to label the contractile ring. Scale bar = 2 μm.

Video 2. ScPFY(9-Mut) drives contractile ring formation in profilin mutant ***cdc3-124*** cells. Related to Figure 3A. Time-lapse (in minutes) of a single Z-plane of *cdc3-124* cells expressing Rlc1-GFP to label contractile rings, and expressing SpPRF, WT ScPFY, or ScPFY(9-Mut). Scale bar = 2 μm.

Video 3. The fission yeast formin Cdc12 nucleates filaments that elongate slowly from their barbed end. Related to Figure 6A and Supplemental Figure 6. TIRF microscopy of actin filaments assembled from 1.5 μM Mg-ATP-actin monomers (33% Oregon green-labeled) in the presence of 5 nM Cdc12(FH1FH2). The barbed end of a control filament is labeled with a red arrowhead, a formin-associated filament is labeled with a green arrowhead.

Video 4. Cdc12-assembled filaments elongate 30-fold faster in the presence of fission yeast profilin SpPRF. Related to Figure 6A and Supplemental Figure 6. TIRF microscopy of actin filaments assembled from 1.5 μM Mg-ATP-actin monomers (33% Oregon green-labeled) in the presence of 5 nM Cdc12(FH1FH2) and 2 μM SpPRF. The barbed end of a control filament (red) and a formin-associated filament (green) are labeled with arrowheads.

Video 5. Cdc12-assembled filaments elongate 10-fold faster in the presence of WT budding yeast profilin ScPFY. Related to Figure 6A and Supplemental Figure 6. TIRF microscopy of actin filaments assembled from 1.5 μM Mg-ATP-actin monomers (33% Oregon green-labeled) in the presence of 5 nM Cdc12(FH1FH2) and 2 μM WT ScPFY. The barbed end of a control filament (red) and a formin-associated filament (green) are labeled with arrowheads.

Video 6. Cdc12-assembled filaments elongate 20-fold faster in the presence of ScPFY(9-Mut). Related to Figure 6A and Supplemental Figure 6. TIRF microscopy of actin filaments assembled from 1.5 μM Mg-ATP-actin monomers (33% Oregon green-labeled) in the presence of 5 nM Cdc12(FH1FH2) and 2 μM ScPFY(9-Mut). The barbed ends of two filaments are labeled with orange arrowheads.

SUPPLEMENTAL REFERENCES

Balasubramanian, M.K., Feoktistova, A., McCollum, D., and Gould, K.L. (1996). Fission yeast Sop2p: a novel and evolutionarily conserved protein that interacts with Arp3p and modulates profilin function. Embo J *15*, 6426-6437.

Basu, R., and Chang, F. (2011). Characterization of dip1p reveals a switch in Arp2/3-dependent actin assembly for fission yeast endocytosis. Curr Biol *21*, 905-916.

Chaudhary, A., Chen, J., Gu, Q.M., Witke, W., Kwiatkowski, D.J., and Prestwich, G.D. (1998). Probing the phosphoinositide 4,5-bisphosphate binding site of human profilin I. Chem Biol *5*, 273-281.

Eads, J.C., Mahoney, N.M., Vorobiev, S., Bresnick, A.R., Wen, K.K., Rubenstein, P.A., Haarer, B.K., and Almo, S.C. (1998). Structure determination and characterization of Saccharomyces cerevisiae profilin. Biochemistry *37*, 11171-11181.

Ezezika, O.C., Younger, N.S., Lu, J., Kaiser, D.A., Corbin, Z.A., Nolen, B.J., Kovar, D.R., and Pollard, T.D. (2009). Incompatibility with formin Cdc12p prevents human profilin from substituting for fission yeast profilin: insights from crystal structures of fission yeast profilin. J Biol Chem *284*, 2088-2097.

Keeney, J.B., and Boeke, J.D. (1994). Efficient targeted integration at leu1-32 and ura4-294 in Schizosaccharomyces pombe. Genetics *136*, 849-856.

Le Goff, X., Motegi, F., Salimova, E., Mabuchi, I., and Simanis, V. (2000). The S. pombe rlc1 gene encodes a putative myosin regulatory light chain that binds the type II myosins myo3p and myo2p. J Cell Sci *113 Pt 23*, 4157-4163.

Liang, D.T., Hodson, J.A., and Forsburg, S.L. (1999). Reduced dosage of a single fission yeast MCM protein causes genetic instability and S phase delay. J Cell Sci *112 (Pt 4)*, 559-567.

Lu, J., and Pollard, T.D. (2001). Profilin binding to poly-L-proline and actin monomers along with ability to catalyze actin nucleotide exchange is required for viability of fission yeast. Mol Biol Cell *12*, 1161-1175.

Neidt, E.M., Scott, B.J., and Kovar, D.R. (2009). Formin differentially utilizes profilin isoforms to rapidly assemble actin filaments. J Biol Chem *284*, 673-684.

Scott, B.J., Neidt, E.M., and Kovar, D.R. (2011). The functionally distinct fission yeast formins have specific actin-assembly properties. Mol Biol Cell *22*, 3826-3839.

Sohn, R.H., Chen, J., Koblan, K.S., Bray, P.F., and Goldschmidt-Clermont, P.J. (1995). Localization of a binding site for phosphatidylinositol 4,5-bisphosphate on human profilin. J Biol Chem *270*, 21114-21120.